

Electronic Supplementary Material (ESI) for Nanoscale.
This journal is © The Royal Society of Chemistry 2020

Electronic Supplementary Information

Potentiated Cytosolic Drug Delivery and Photonic Hyperthermia by 2D Free-Standing Silicene Nanosheets for Tumor Nanomedicine

*Fangfang Wang,^{a†} Huican Duan,^{a†} Ruifang Zhang,^{*a} Haiyan Guo,^a Han Lin^{*b} and Yu Chen^{*b,c}*

Experimental Figures

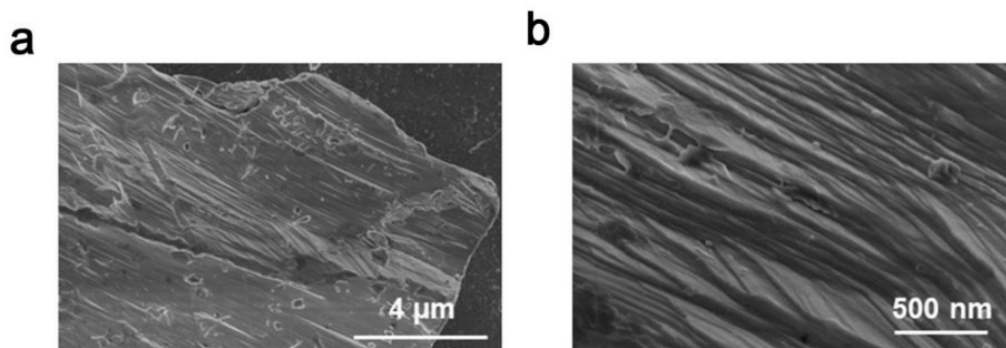


Figure S1. SEM images of Zintl phase CaSi_2 precursor before liquid oxidation and exfoliation at (a) low and (b) high magnifications, which are high magnification images of Figure 1a.

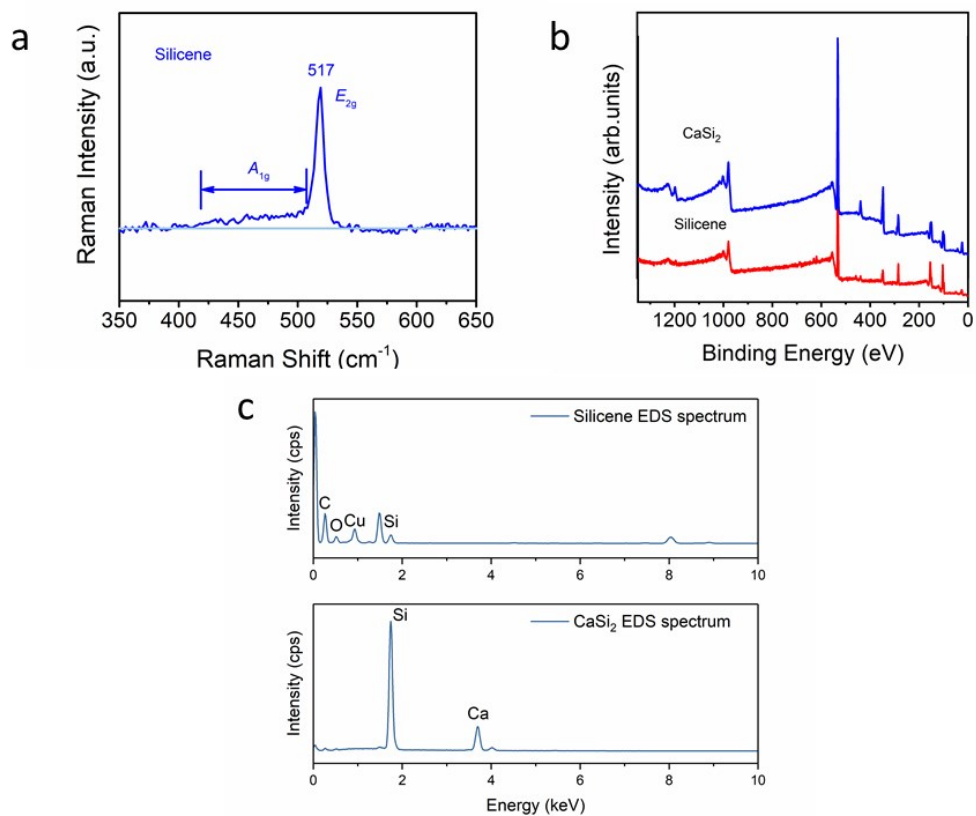


Figure S2. (a) Raman spectrum of as-fabricated product (silicene nanosheets). (b) XPS spectra of CaSi₂ powder and silicene nanosheets in the region containing all possible elements. (c) EDS profiles of the precursor CaSi₂ and product silicene nanosheets.

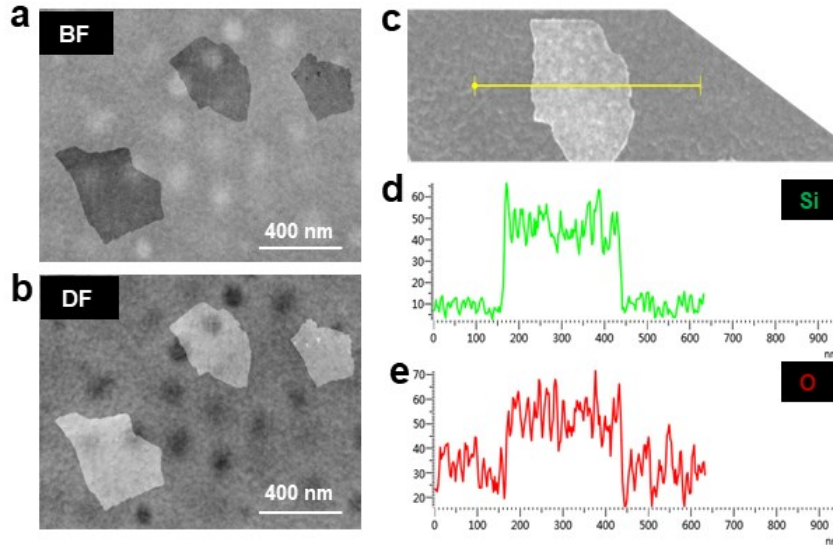


Figure S3. (a) Bright-field TEM image, (b) dark-field TEM image, and (c-e) the corresponding element-linear scanning images of 2D silicene nanosheets.

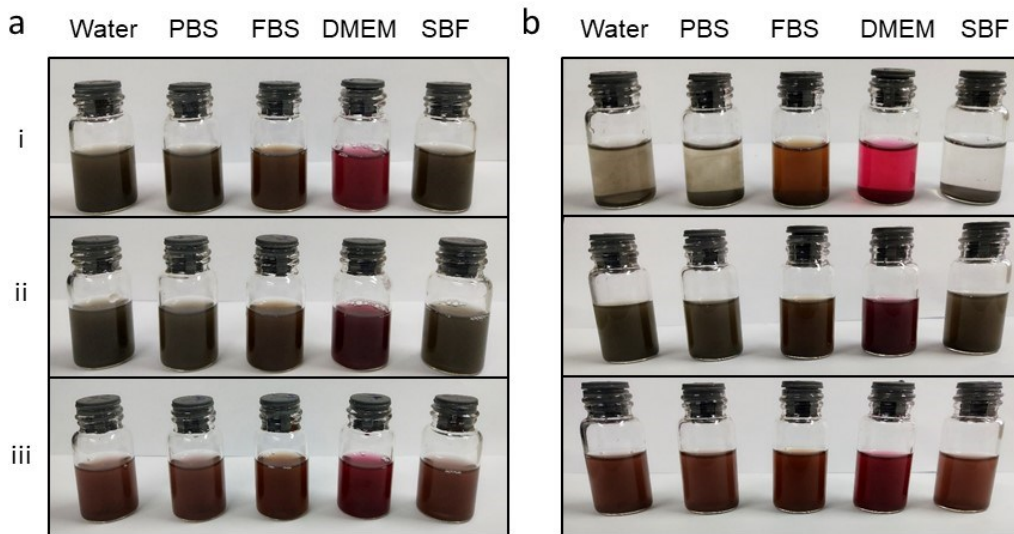


Figure S4. Digital photographs of (i) silicene NSs, (ii) silicene-BSA NSs, and (iii) DOX@silicene-BSA NSs dispersed in water, PBS, FBS, DMEM and SBF with time intervals of (a) 0 h and (b) 24 h.

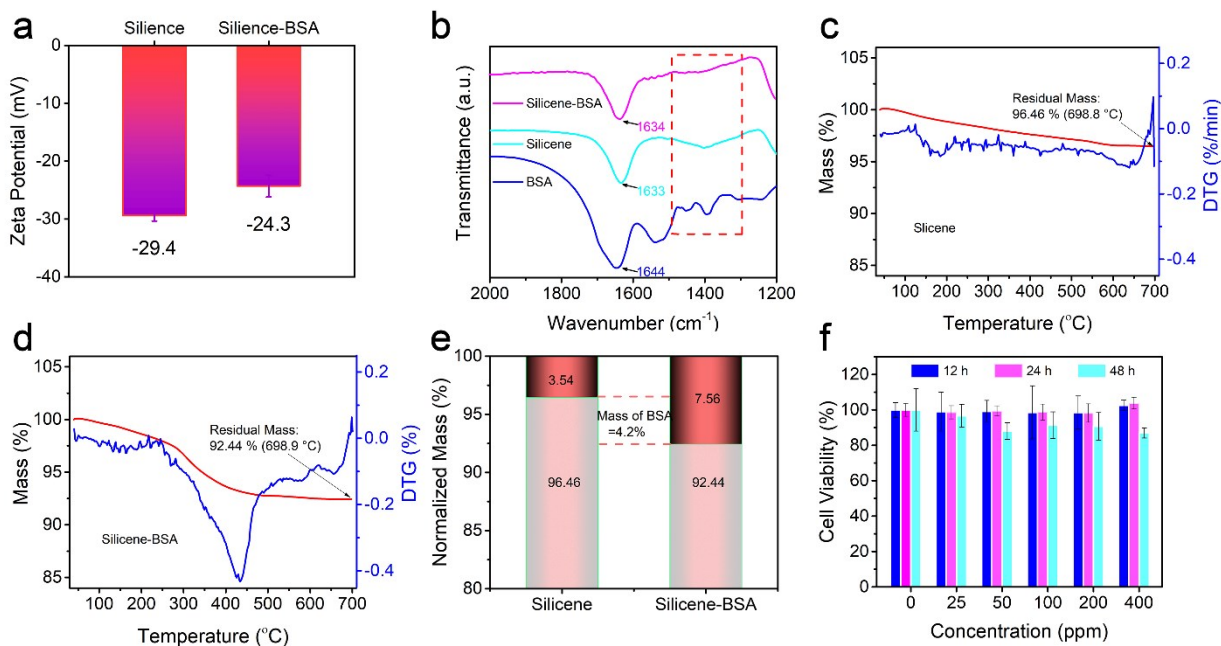


Figure S5. (a) Zeta potentials of silicene and silicene-BSA NSs dispersed in water. (b) FT-IR spectra of silicene NSs, BSA, and silicene-BSA NSs. Thermogravimetric analysis (TGA) curves of (c) silicene NSs and (d) silicene-BSA NSs. (e) Normalized weight loss distribution diagrams of silicene and silicene-BSA NSs. (f) 4T1 cells viabilities after incubation with silicene-BSA NSs at varied concentrations (0, 25, 50, 100, 200, and 400 $\mu\text{g/mL}$) for varied time intervals (12, 24, and 48 h).

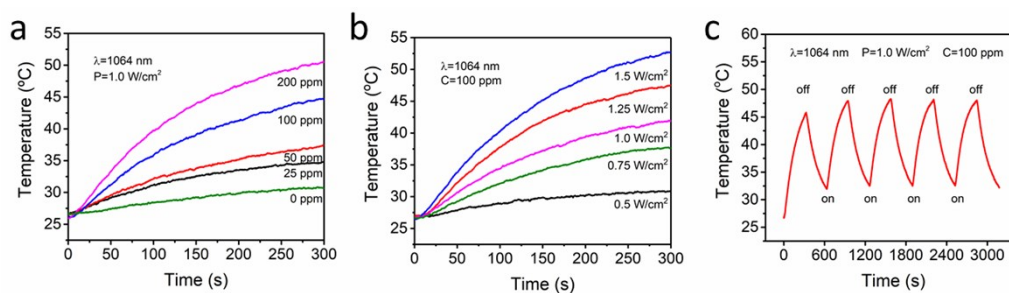


Figure S6. (a) Photothermal-heating curves of silicene-BSA NSs aqueous solution at different concentrations (0, 25, 50, 100, and 200 $\mu\text{g/mL}$) exposed to a NIR-II laser (1064 nm) at the power intensity of 1 W/cm^2 for 5 min. (b) Photothermal-heating curves of silicene-BSA NSs aqueous solution at the concentration of 100 $\mu\text{g/mL}$ exposed to a NIR-II laser (1064 nm) at varied power intensities (0.5, 0.75, 1.0, 1.25, and 1.5 W/cm^2) for 5 min. (c) Cycling heating and cooling curves of silicene-BSA NSs aqueous solution (100 $\mu\text{g/mL}$) exposed to an 1064 nm NIR laser (1 W/cm^2) for five cycles of NIR-II laser on/off.

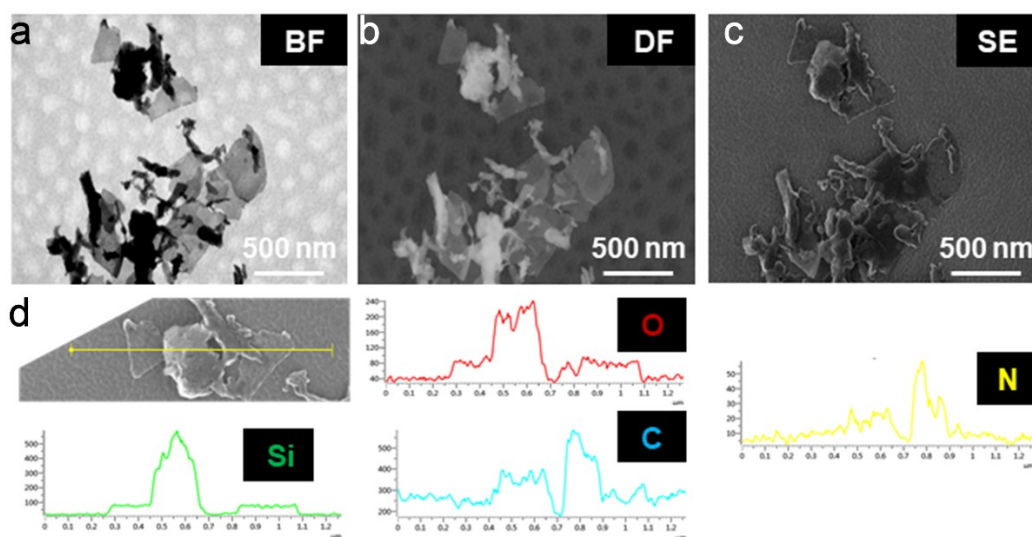


Figure S7. (a) Bright-field TEM image, (b) dark-field TEM image, (c) secondary electron SEM image, and (d) the corresponding element-linear scanning images of DOX@silicene-BSA NSs.

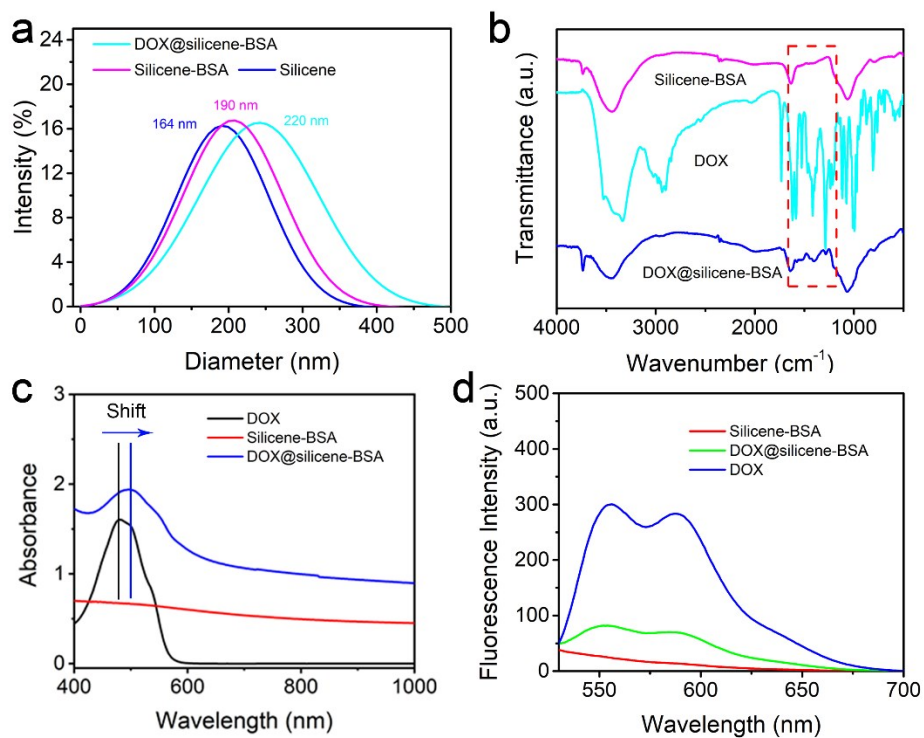


Figure S8. (a) Size distribution of silicene, silicene-BSA and DOX@silicene-BSA NSs dispersed in water. (b) FT-IR spectra of DOX, silicene-BSA NSs, and DOX@silicene-BSA NSs. (c, d) Absorption spectra and fluorescence spectra ($\lambda_{\text{ex}} = 480 \text{ nm}$, $\lambda_{\text{em}} = 570 \text{ nm}$) of DOX molecules after being loaded on the silicene-BSA NSs.

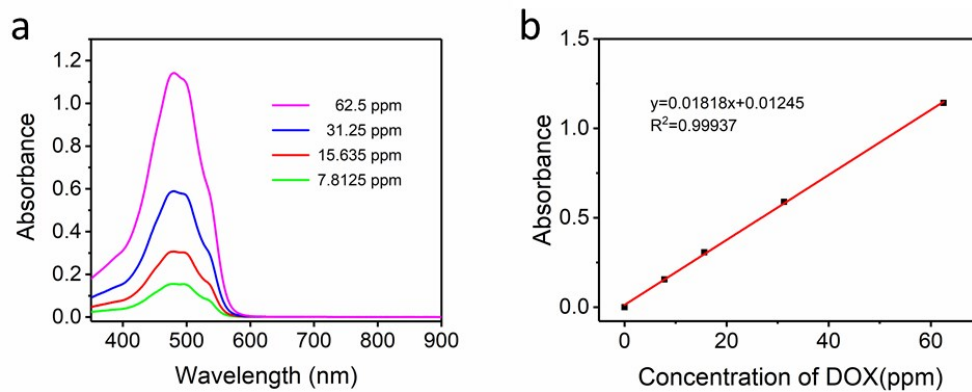


Figure S9. (a) Absorbance of DOX aqueous solution at elevating concentrations. (b) Normalized absorbance values of DOX at the wavelength of 480 nm.

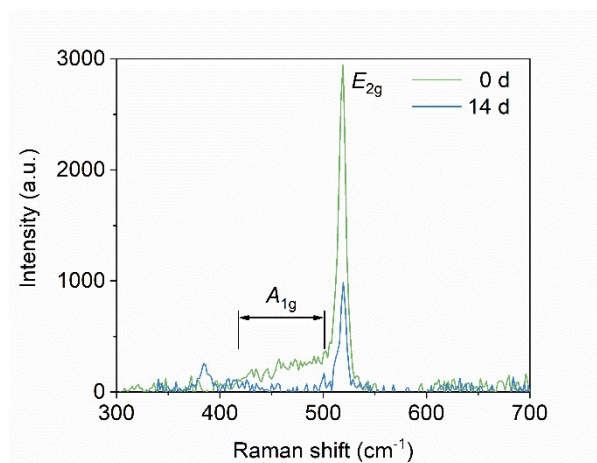


Figure S10. Raman spectra of DOX@silicene-BSA suspension in the physiological medium (PBS) at room temperature (RT) for 0 day and 14 days.

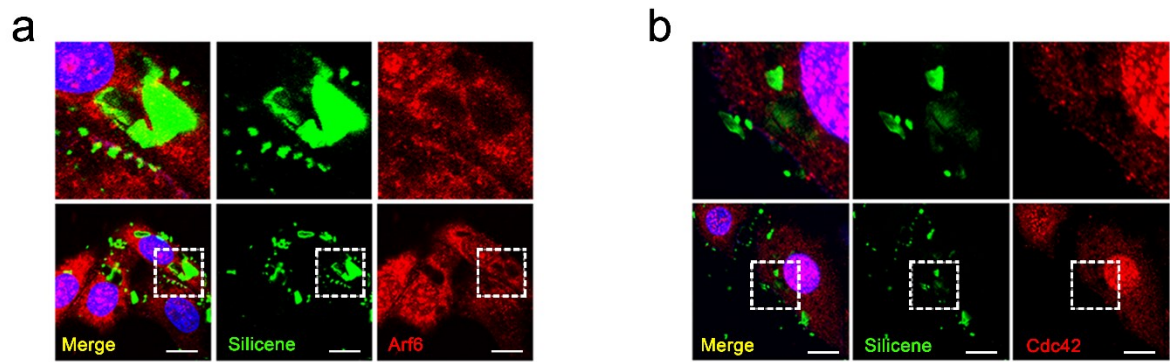


Figure S11. CLSM images of 4T1 cells treated with FITC-labeled silicene-BSA NSs. The primary antibody against (a) Arf6 and (b) Cdc42 were used to detect the immunofluorescence (Scale bars: 10 μm).

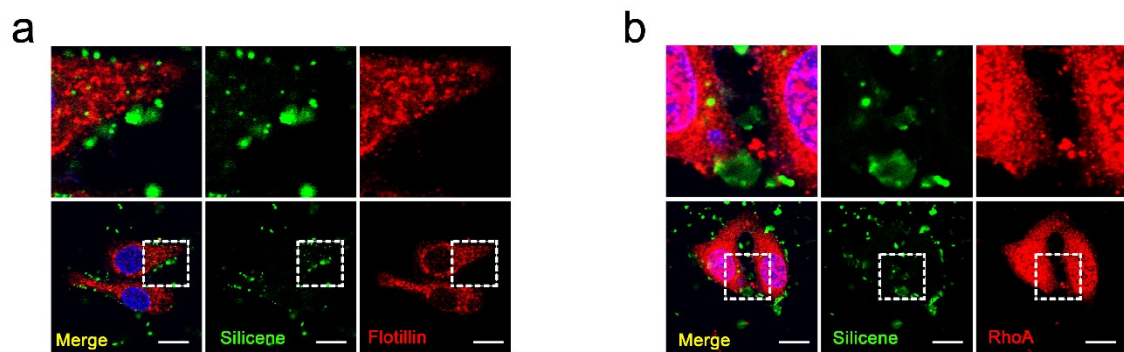


Figure S12. CLSM images of 4T1 cells treated with FITC-labeled silicene-BSA NSs. The primary antibody against (a) Flotillin and (b) RhoA were used to detect the immunofluorescence (Scale bars: 10 μm).

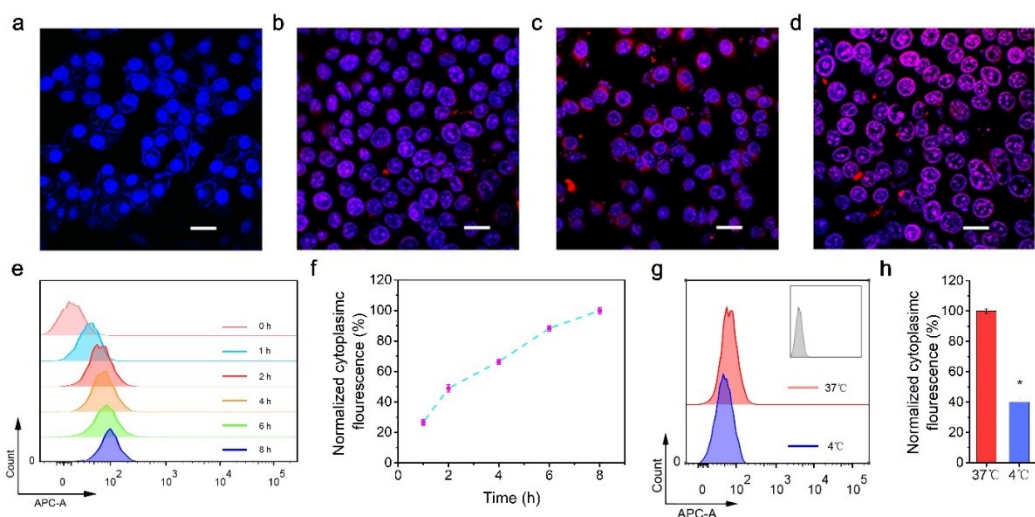


Figure S13. (a-d) CLSM images of 4T1 cancer-cell line treated by DOX-loaded silicene-BSA NSs at varied time intervals of incubation (0, 1, 2, and 4 h) (Scale bars: 20 μm). (e) Cellular uptake analysis of DOX@silicene-BSA NSs by flow cytometric assay at varied incubation time intervals (0, 1, 2, 4, 6, and 8 h). (f) Statistical analysis of fluorescence for 4T1 cell cytoplasm at the corresponding time intervals. (g) Temperature (37 $^{\circ}\text{C}$ and 4 $^{\circ}\text{C}$) effects on the cellular uptake of DOX@silicene-BSA NSs after 1 h incubation. (h) Histogram of cytoplasmic fluorescence. (Scale bar: 10 μm ; *P < 0.05).

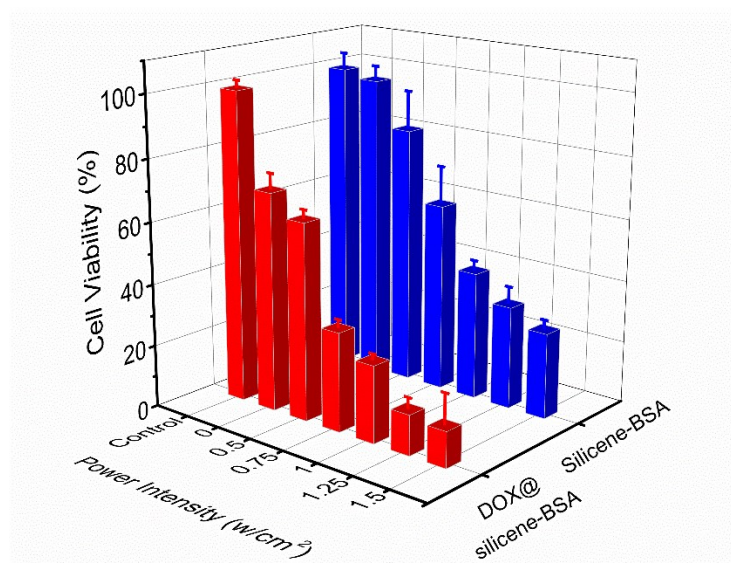


Figure S14. Cell viabilities of 4T1 cells after treatment with silicene-BSA or DOX@silicene-BSA NSs (silicene-BSA: 60 $\mu\text{g/mL}$) at varied laser power densities (0~1.5 W/cm^2) for 5 min.

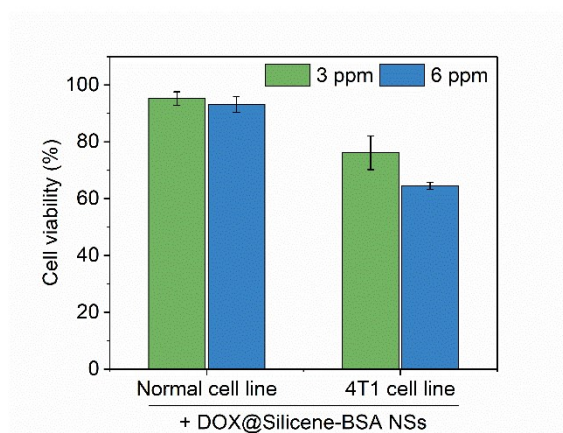


Figure S15. Cell viabilities of normal cell line and 4T1 cell line after treatment with DOX@silicene-BSA NSs (DOX: 3 or 6 $\mu\text{g/mL}$).

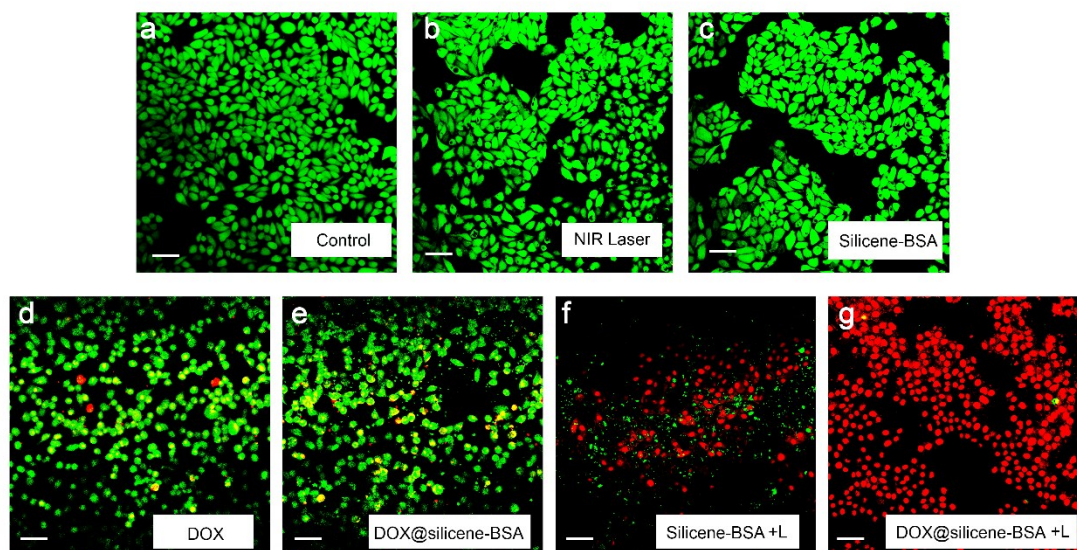


Figure S16. CLSM images of 4T1 cells treated with different treatments before calcein-AM/PI co-staining (Scale bars: 50 μm).

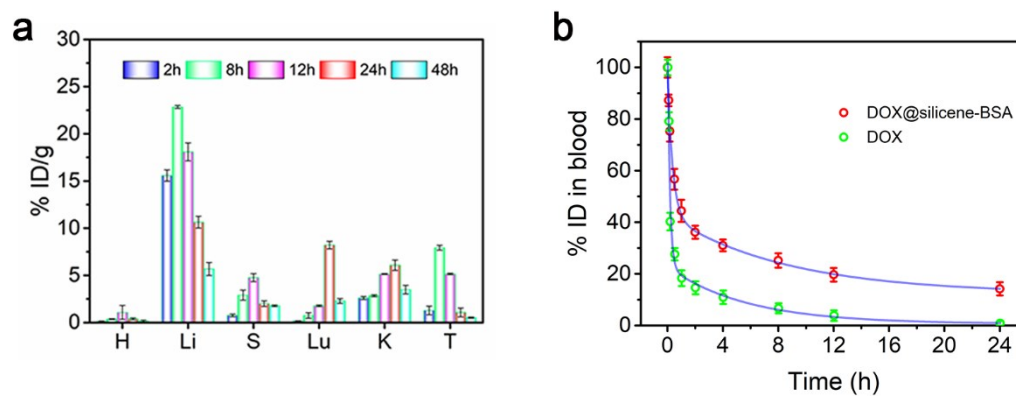


Figure S17. (a) Quantitative biodistribution analysis of Si in major organs and tumor by ICP-OES at different time intervals of 2, 8, 12, 24, and 48 h after intravenous administration of DOX@silicene-BSA NSs (n = 3). (b) Pharmacokinetics of free DOX and DOX@silicene-BSA NSs after intravenous injection into the 4T1 tumor-bearing mice (n = 3). The blood circulation curve of free DOX and DOX@silicene-BSA NSs determined by measuring the DOX fluorescence intensity in the blood samples.

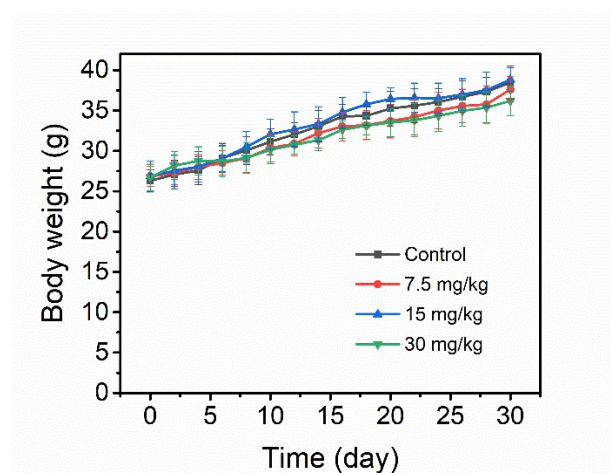


Figure S18. Body weights of KM mice with the injection of different doses of silicene-BSA NSs dispersed in PBS (0, 7.5, 15, and 30 mg/kg) to assess the biocompatibility and biosafety for one-month period (n = 5, mean \pm SD).

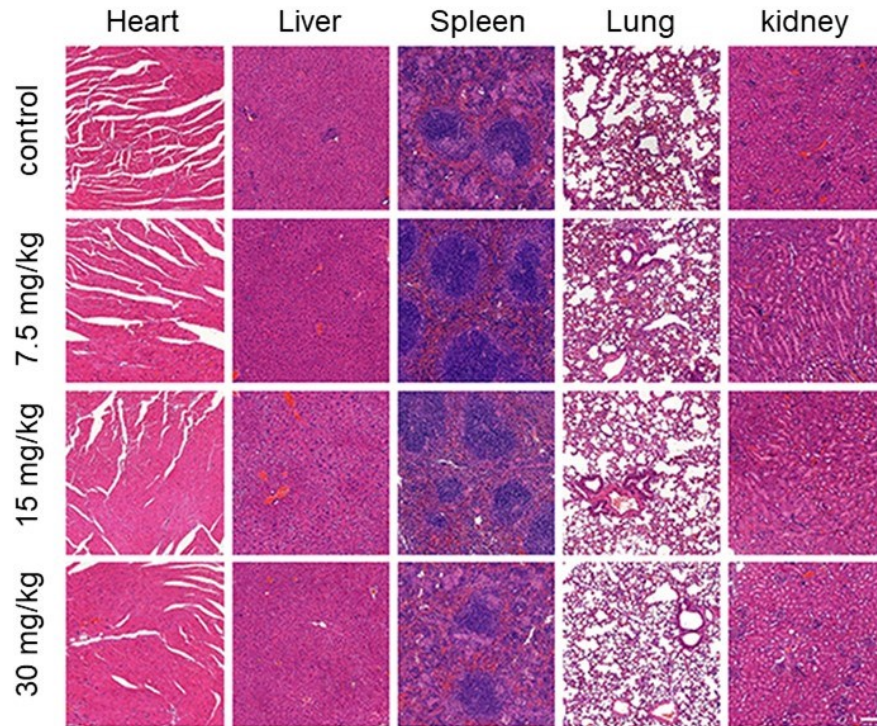


Figure S19. Histological images of H&E staining tissue sections dissected from main organs (*i.e.* heart, liver, spleen, lung and kidney) to assess the *in vivo* biosafety after injection for 30 days with various treatments (Share scale bar = 100 μ m).

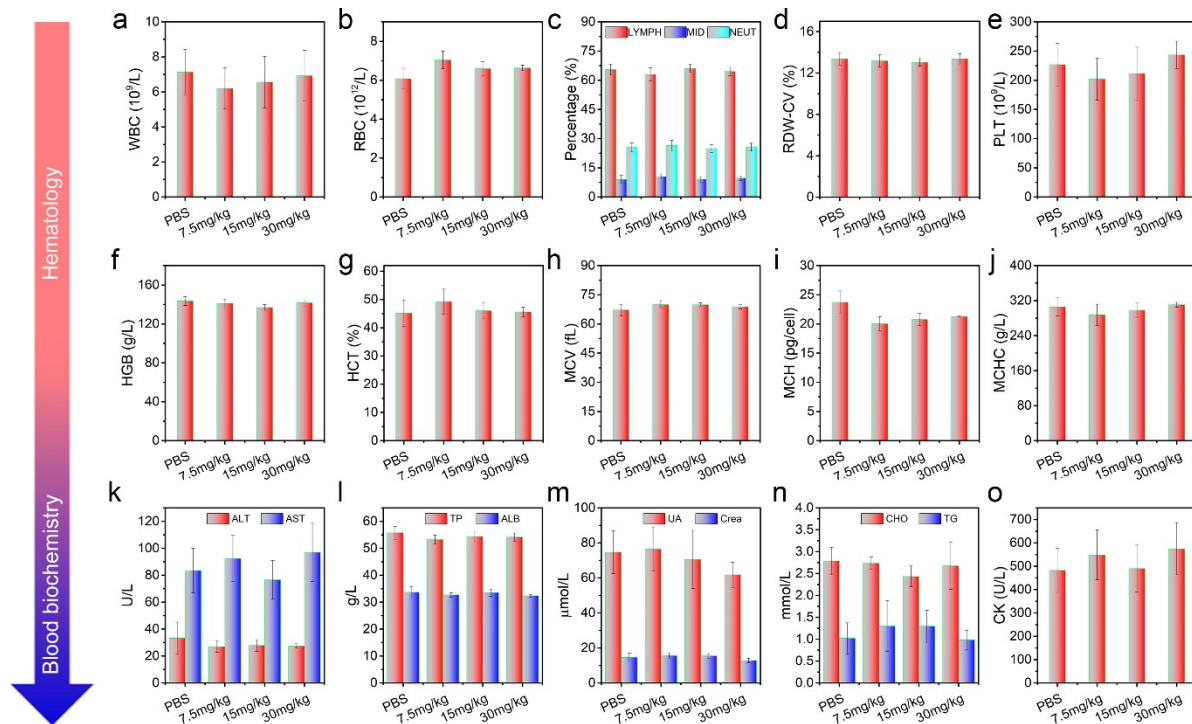


Figure S20. Hematology and blood biochemistry index of KM mice treated with different doses of silicene-BSA NSs (0, 7.5, 15, and 30 mg/kg). The parameters were collected at one month post-injection: (a) white blood cells (WBC), (b) red blood cells (RBC), (c) percentage of lymphocyte (LYMPH), intermediate cells (MID) and neutrophil (NEUT), (d) coefficient of variation of red blood cell distribution width (RDW-CV), (e) platelet (PLT), (f) hemoglobin (HGB), (g) hematocrit (HCT), (h) mean corpuscular volume (MCV), (i) mean corpuscular hemoglobin (MCH), (j) mean corpuscular hemoglobin concentration (MCHC), (k) alanine aminotransferase (ALT) and aspartate aminotransferase (AST), (l) total Protein (TP) and albumin (ALB), (m) uric acid (UA) and creatinine (Crea), (n) cholesterol (CHO) and triglyceride (TG), and (o) creatine kinase (CK). The above values are shown as mean and s.d..

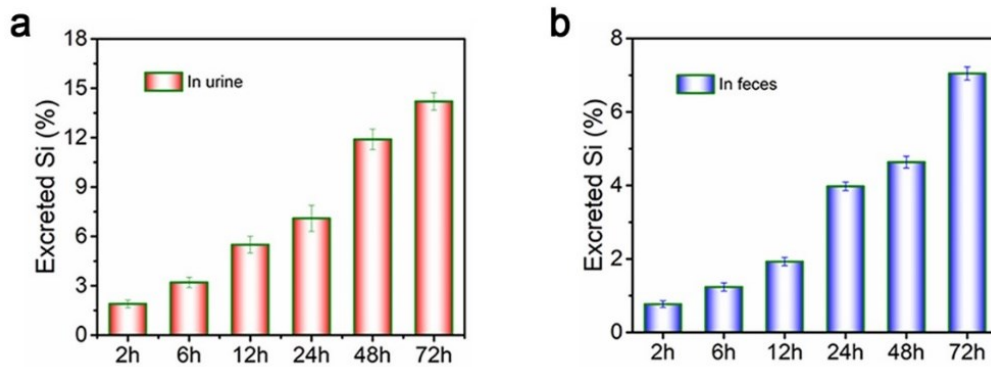


Figure S21. Accumulated Si in (a) urine and (b) feces for excretion out of KM mice after the post-injection of DOX@silicene-BSA NSs (n = 3) for varied durations (2, 6, 12, 24, 48, and 72 h).

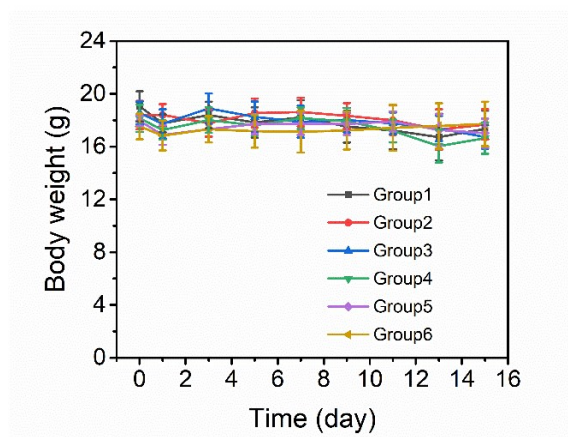


Figure S22. The body weight change of 4T1 tumor-bearing nude mice during different treatments. Six treatment groups include control (Group 1), NIR-II laser (Group 2), free DOX (Group 3), DOX@silicene-BSA (Group 4), silicene-BSA + NIR-II laser (Group 5), and DOX@silicene-BSA + NIR-II laser (Group 6) (n=6).